The Optimal k-Covering Tag Deployment for RFID-based Localization ☆

Wei-Shinn Ku[a,1], Kazuya Sakai[a], Min-Te Sun[b]

[a]*Department of CSSE, Auburn University, Auburn, AL 36849, USA*
[b]*Department of CSIE, National Central University, Taoyuan 320, Taiwan*

Abstract

Radio Frequency Identification (RFID) technologies are applied in many fields for a variety of applications today. Recently, new solutions are proposed to deploy RF tags on the ground instead of attaching them to objects for RFID-based monitoring and localization. However, the optimal tag deployment strategy is yet to be addressed. In this paper, we identify the optimal deployment patterns that guarantee k-covering (i.e., at least k RFID tags are accessible anywhere in the deployment region), where $k \leq 3$. In addition, we analyze the achievable minimum upper bound and the average of localization error when the optimal deployment patterns are applied. The numerical results show that our optimal deployment patterns significantly reduce the required number of tags for k-covering compared with the square pattern which is commonly used in RFID-based monitoring and localization systems. The comparison between simulation and analytical results shows that our analytical models provide very accurate estimations of localization error.

---

[*]Corresponding author: Min-Te Sun
E-mail address: msun@csie.ncu.edu.tw

1. Introduction

Radio Frequency Identification (RFID) is an electronic tagging technology that allows objects to be automatically identified at a distance using an electro-magnetic challenge-and-response exchange of data (Want, 2004). By attaching Radio Frequency (RF) tags to objects, RFID technologies enable various applications such as supply chain management (Santos and Smith, 2008), transportation payment, warehouse operations (Chow et al., 2006), library management (Boss, 2003), indoor location sensing (Liu et al., 2007), and so on.

Recently, new types of RFID-based applications such as activity monitoring and localization have been proposed. In these applications, RF tags are deployed in a region instead of attaching them to objects. For example, in (Liu et al., 2007), a few RF readers continuously monitor signal strength of deployed RF tag arrays for identifying frequent trajectories of moving objects. This system can be employed to replace expensive camera-based activity monitoring techniques. Similarly, in (Mitchell et al., 2009; Munishwar et al., 2009b), an iRobot Create (iRobotCreate, 2009) is equipped with RF readers and passive RF tags are deployed in a testbed field. By reading tag identification information, the robot can locate its current position. It has been shown that the RFID-based solution is capable of providing more accurate localization than sensor-based localization mechanisms. Although these systems support practical applications, they did not consider how to optimize the tag deployment so that the number of required RF tags can be minimized. Currently, the square pattern is commonly used to deploy RF tags for RFID-based localization and monitoring. While the square pattern is

2

an intuitive way to deploy tags, it is not the optimal deployment pattern. Even though the unit price of RF tags is relatively cheap, the cost of a vast amount of tags is still significant. In addition, the relationship between localization error and tag deployment pattern has never been studied.

In this research, we investigate the optimal k-covering tag deployment patterns, which are defined as the deployment patterns that result in the least number of RF tags to cover a region with a given minimal number of tags k that a reader can access anywhere in the region. The contributions of this research are as follows:

- We identify the optimal k-covering tag deployment patterns for $k \in \{1, 2, 3\}$. When $k = 1$, the deployment problem is essentially identical to the minimum cover set problem (Kershner, 1939). It is known that the equilateral triangle pattern with edge length $\sqrt{3}r$ is optimal, where r is the readable range of a tag. For $k = 2$ and $k = 3$, we prove the hexagon pattern with edge length r and the diamond pattern with edge length r are optimal, respectively.

- We analyze the achievable minimum upper bound of localization error when our optimal k-covering tag deployment patterns are applied. The localization error is upper bounded by r when $k = 1$, by $\frac{\sqrt{3}}{2}r$ when $k = 2$, and by $\frac{1}{2}r$ when $k = 3$.

- We design the analytical models of the average localization error when the optimal deployment patterns are applied for the three k values.

- To evaluate the performance, numerical evaluation and extensive simulations are conducted. The results show that our optimal k-covering deploy-

ment patterns require only 77%, 87%, and 58% of the amount of tags which are required by the commonly used square pattern, for $k = 1$, $k = 2$, and $k = 3$, respectively. The comparison between simulation and analytical results shows that our analytical models provide very accurate estimations of localization error.

The remainder of this paper is organized as follows. Section 2 surveys the related work. Section 3 introduces the motivation and problem formulation. The optimal k-covering deployment patterns and the proofs of optimality are presented in Section 4. In Section 5, we present the analysis for the upper bound and the average of localization error. The numerical and simulation results are demonstrated in Section 6. Section 7 concludes this paper.

2. Related Work

2.1. RFID-based Object Monitoring

RFID systems consist of RF readers and RF tags. RF tags can be classified into two types, active tags and passive tags. An active tag contains a radio transceiver and its own power source. Generally, active tags are expensive and may not be suitable for applications which require a large number of tags. On the other hand, a passive tag exchanges data with RF reader through an electromagnetic challenge-and-response manner. Since passive tags require no battery, they are rather inexpensive and relatively affordable for large-scale deployment.

By attaching RF tags to moving objects, there are various RFID-based object monitoring applications such as supply chain management (Santos and Smith, 2008), transportation payment, library management (Boss, 2003), animal identification, warehouse operations (Chow et al., 2006), etc. These applications sig-

nificantly facilitate our daily life and bring great productivity gains. For example, RFID technology was introduced to automate library operations (Boss, 2003) by attaching passive tags to books. The authors of (Xie et al., 2008) proposed a sampling-based approach for information recovery that can identify which shelf a certain book is located.

In all of the aforementioned applications, RF tags are attached to objects. A recent research utilized RF tags for mining frequent trajectory patterns for activity monitoring by deploying an array of active tags onto the field (Liu et al., 2007). When an object moves through the field, the signals from some active tags will be affected and the RF readers will receive such signals. A database server collects the changes of signal strength and then derives the activities in the field. Their experimental results show that employing RF tags to find trajectories of frequent activities is highly feasible.
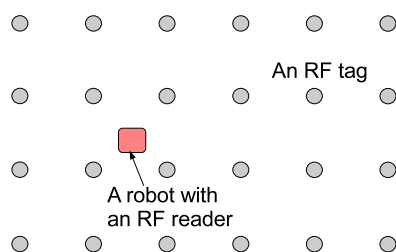
2.2. RFID-based Object Localization

Figure 1: RFID-based localization.

Among all the RFID-based applications, RFID-based object localization (Choi et al., 2006; Jin et al., 2006; Munishwar et al., 2009a) is the primary application of this research. In this RFID-based object localization system, numerous RF tags are deployed in a region with their unique identifiers. When a moving object (e.g.,

a robot) with an RF reader reads the identifier of a tag, it can obtain the location of the tag from the database. This enables the moving object to calculate its current location as illustrated in Figure 1.

In (Mitchell et al., 2009; Munishwar et al., 2009b), the authors proposed an accurate and inexpensive RFID-based localization mechanism for the iRobot Create platform (iRobotCreate, 2009), which is a programmable robot primarily designed for robotics development. In their system, robots are equipped with RF readers and passive tags are deployed in a testbed region. Generally, a robot calibrates its location and orientation using the coordinates of the first and latest encountered tags on a straight line movement. They demonstrated that the RFID-based localization scheme results in lower localization error than the sensor-based localization scheme. The related work closest to ours is presented in (Choi et al., 2006) which focuses on achieving accurate localization using RFID for Cellular Phone Robot (CPR). They studied how to distribute RF tags (i.e., tag pattern) and how many tags to place (tag granularity) on the floor to accomplish efficient navigation with three different tag deployment patterns. Nevertheless, their solution cannot compute the optimal deployment pattern for an arbitrary region with user-defined parameters.

3. Motivation and Problem Formulation

3.1. Motivation

In the aforementioned RFID-based applications such as object monitoring and localization, the square pattern is commonly used to deploy RF tags in the field. In practice, the square pattern is a very intuitive way to deploy tags, but not the most efficient pattern. Although the unit price of RF tags is low, a large number

6

of tags are required to cover a given region as RF tags have a limited read range. Hence, the optimal tag deployment pattern which requires the least number of tags to cover the region is definitely of interest.
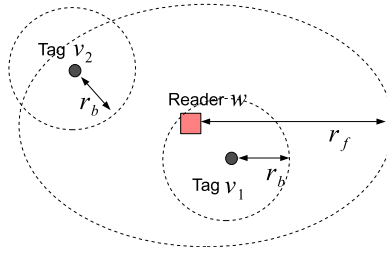
3.2. Problem Formulation

Figure 2: An example of tag access.

Similar to traditional wireless networks, we model an RFID system as a graph $G = \{V, E\}$. Here, V is a set of vertices, which includes the set of tags $\{v_i\}$ and the set of readers $\{w_j\}$. E is the set of edges, where each edge represents the link between a tag and a reader if they are within proximity of each other. Let r_f denote the forward channel range (i.e., the transmission range from a reader to a tag) and r_b the backward channel range (i.e., the transmission range from a tag to a reader). Generally, the forward channel range is much longer than the backward channel range, as shown in Figure 2. Only when the distance between a tag and a reader is less than $\min\{r_f, r_b\}$, is the reader able to access tag data. Thus, we define $r = \min\{r_f, r_b\}$ as the communication range and C_i as the readable area of a tag v_i, which is modeled as a circle with radius r centered at the location of v_i.

Consider the case that a number of tags are deployed in a region, and there is no reader. As passive tags do not have their own power source, they cannot

7

communicate with each other. A tag can send its identifer, only when a reader sends an interrogation signal. Hence, the graph is now $G = \{V, \phi\}$, where $V = \{v_1, v_2, ..., v_k\}$. Let a robot with an RF reader w join the network. Assuming the reader w is within the readable area of both v_1 and v_2, the graph will be $G = \{V, E\}$, where $E = \{< w, v_1 >, < w, v_2 >\}$ and $|E| = 2$. Consequently, the reader can estimate its current location from the locations of tag v_1 and v_2.

It is clear that a random deployment of passive tags is not efficient, and a planned deployment such as the square pattern is a cost-effective way to guarantee the coverage of a region with fewer tags. For better localization, we are interested in finding the tag deployment pattern that a reader can access at least k tags at any point in the deployment region with the least total number of tags. In the following, we formally define the optimal k-covering tag deployment pattern.

Definition 1 *The optimal k-covering tag deployment pattern is defined as the pattern that a reader can access at least k tags at any point in the deployment region with the least total number of tags.*

Now the problem addressed by this research can formally be formulated as follows.

Definition 2 *The optimal k-covering tag deployment problem is to identify the optimal k-covering tag deployment pattern.*

The optimal tag deployment pattern can be applied to various RFID-based applications, such as RFID-based object localization. Note that the optimal tag deployment pattern is not meant to minimize the localization error. This is because achieving low localization error is equivalent to deploying as many tags as possible. At first glance, the problem is similar to the minimum cover set

problem (Kershner, 1939) and the sensor cover problem (Bai et al., 2006). The minimum cover set problem is to find the optimal pattern to cover a given region by circles with a given radius. While the minimum cover set problem is a pure mathematical problem, the sensor cover problem incorporates practical considerations for wireless sensor networks. In the sensor cover problem, a sensor node has both a sensing range and a communication range. The sensor deployment pattern not only covers a region by the sensing range of sensor nodes, but also considers the connectivity of sensor nodes with their communication range. As far as we know, deployment patterns of sensor nodes for full-sensing-coverage and up to 6-connectivity were proposed and their optimalities were proved (Bai et al., 2006, 2008). The main difference between these problems and this research is that they do not consider overlaps of circles (i.e., k-covering), which is the primary concern for RFID-based localization. For ease of reference, the notations used in this paper are summarized in Table 1.

4. The Optimal RFID Deployments

In this section, we investigate the optimal k-covering tag deployment patterns for $k \in \{1, 2, 3\}$. When $k = 1$, the problem is identical to the minimum cover set problem (Kershner, 1939), in which the equilateral triangle with edge length $\sqrt{3}r$ is optimal. When $k = 2$ and $k = 3$, we discover that the hexagon pattern with edge length r and the diamond pattern with edge length r are optimal, respectively. In addition to the optimal tag deployment patterns, we also analyze the square pattern, since it is a deployment pattern commonly used in RFID-based localization applications.

9

Table 1: Notations.

Symbol	Definition
v_i	RFID tag i
w_j	RFID reader w_j
r_f	The forward channel range
r_b	The backward channel range
r	The communication range, $\min\{r_f, r_b\}$
R	The tag deployment region
k	The least number of tags that a reader can access at any point in R
C_i	The readable area of tag v_i
$|C|$	When the Unit Disk Graph model is employed, $\forall i \; |C_i| = |C|$
N	The total number of tags to be deployed
$I(p)$	The indication function at location p
W_i	The weighted covering of readable area of tag v_i
$Intc(p)$	The indication function of coverage intersection at location p
$L(p)$	The weighted covering indication function at point p
L	The weighted covering area off all tags
L'	The weighted area covered by more than k tags
Err	The localization error
Err_{up}	The upper bound of Err
$\overline{Err_k}$	The average error for the optimal k-covering tag deployment pattern
(x_e, y_e)	The estimated location
d	The Euclidean distance between two points

4.1. Assumptions

The signal of an RF reader is usually directional. However, as presented in (Munishwar et al., 2009b; Mitchell et al., 2009; Ota et al., 2008), a robot is equipped with multiple antennas and sends an interrogation signal several times in all directions. Therefore, in this research, we assume that signals from a reader are ideally sectorized and the number of sectors is infinity, i.e., the unit disk graph.

4.2. The Optimal Tag Deployment Pattern for $k = 1$

To access an RF tag, the distance between a tag and a reader must be less than the communication range. Let C_i denote the disk of the readable area of tag v_i. When $k = 1$, a reader has to access at least one tag at any point in the deployment region R. Therefore, the deployment pattern must satisfy Equation 1.

$$R \subseteq \bigcup_{\forall i} C_i \tag{1}$$

Let N be the total number of tags deployed in R. From Definition 2, our goal is to minimize N while at the same time satisfying Equation 1. This is essentially the same problem as the minimum cover set problem (Kershner, 1939). Therefore, we can derive the following theorem:

Theorem 1 *When $k = 1$, the optimal RFID tag deployment pattern is the equilateral triangle pattern with edge length $\sqrt{3}r$.*

Proof 1 *The detailed proof of Theorem 1 can be found in (Kershner, 1939; Zhang and Hou, 2005).*

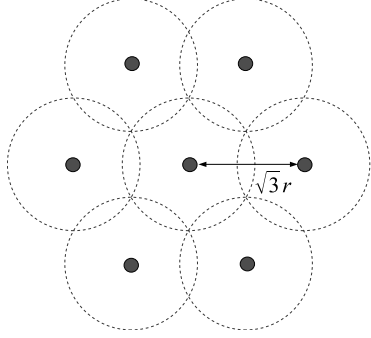The equilateral triangle pattern is shown in Figure 3.
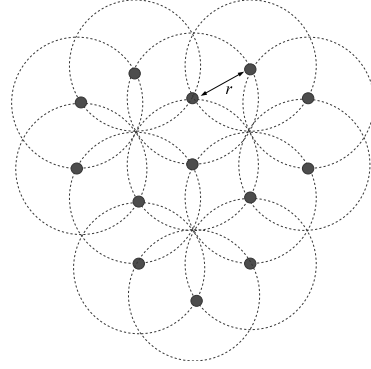
Figure 3: The optimal pattern for $k = 1$.   Figure 4: The optimal pattern for $k = 2$.

4.3. The Optimal Tag Deployment Pattern for $k = 2$

To enable an RF reader to access at least two tags at any point in the deployment region R, the readable area of all tags should cover the whole region R twice. Let $Intc_i$ denote the intersection of readable area between tag v_i and any other tag, the deployment must satisfy following:

$$R \subseteq \bigcup_{\forall i} Intc_i \tag{2}$$

Under the assumption of the unit disk model, $\forall i \, |Intc_i| = |C_i| = |C|$. When $k = 2$, we observe that the hexagon pattern is optimal. To prove this, we show that minimizing the number of tags to be deployed is equivalent to minimizing the amount of area covered by more than 2 tags.

Theorem 2 *Given the requirement of k-covering, minimizing the number of tags to be deployed in the region R is equivalent to minimizing the amount of area that is covered by more than k tags.*

Proof 2 *To prove the theorem, we illustrate that the relationship between the num-*

12

ber of deployed tags and the weighted covering area is linear to each other with a positive slope. First, let us introduce an indication function $I_i(p)$, which is defined by Equation 3.

$$I_i(p) = \begin{cases} 1, & if \ p \in C_i \\ 0, & otherwise \end{cases} \tag{3}$$

The weighted covering of the readable area of tag v_i is defined as follows.

$$W_i = \int_{p \in R} \sum_{j=i+1}^{N} I_i(p) \cdot I_j(p) dx \quad , (i \neq j) \tag{4}$$

Let us denote the average weighted covering of the readable area as $\overline{W}$, which is defined as follows.

$$\overline{W} = \frac{1}{N} \sum_{i=0}^{N} W_i \tag{5}$$

The weighted covering indication function at point p, $L(p)$, is defined as:

$$L(p) = \sum_{i=0}^{N} \sum_{j=i+1}^{N} I_i(p) \cdot I_j(p) \quad (i \neq j) \tag{6}$$

Equation 6 shows the number of tags covering the point p minus one. For example, in Figure 5, the point p_1 is only covered by the readable area of one tag and therefore $L(p_1) = 0$. On the other hand, the point p_2 is 3-covering and thus $L(p_2) = 2$. The weighted covering of all tags, L, is obtained as follows.

$$L = \int_{p \in R} L(p) dp \qquad (7)$$

$$= \int_{p \in R} \left(\sum_{i=0}^{N} \sum_{j=i+1}^{N} I_i(p) \cdot I_j(p) \right) dp \qquad (8)$$

$$= \sum_{i=0}^{N} \left(\int_{p \in R} \sum_{j=i+1}^{N} I_i(p) \cdot I_j(p) dp \right) \qquad (9)$$

$$= \sum_{i=0}^{N} W_i \qquad (10)$$

$$= N\overline{W} \qquad (11)$$

From the system requirement, all points in R have to be covered by at least k tags, hence $\forall p \ L(p) \geq (K-1)$. The area covered by more than k tags, denoted as L', is obtained by the following formula:

$$L' = L - (K-1) \int_R dp = N\overline{W} - (K-1)|R| \qquad (12)$$

Equation 12 shows that the amount of area covered by more than k tags and the number of tags have a linear relationship with a positive slope. This concludes the proof.

With Theorem 2 in place, we are now ready to prove that our hexagon pattern is optimal when $k = 2$.

Theorem 3 *The optimal 2-covering RFID tag deployment pattern is hexagon with edge length r.*

Proof 3 *To satisfy Equation 2, each point in R needs to be covered by at least two tags. Consider a set of tags $\{v_0, v_1, v_2, ..., v_n\}$ and their readable areas*
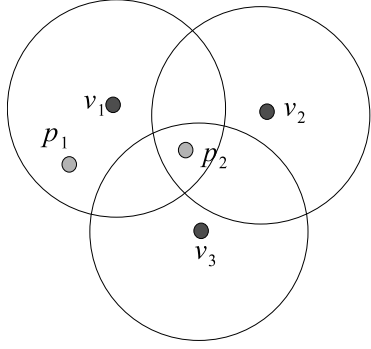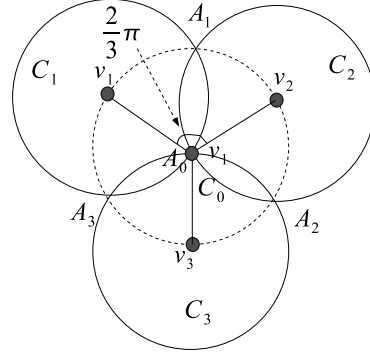
14

Figure 5: Weighted covering area.

Figure 6: An example for the proof when $k = 2$.

$\{C_0, C_1, C_2, ..., C_n\}$, *which are illustrated in Figure 6. The issue is that how many neighboring tags, denoted by* n, *are required to cover* C_0 *and at the same time result in the minimum area covered by more than 2 tags. We consider the following two disjoint cases: 1) when* $n < 3$ *and 2) when* $n \geq 3$.

Case 1 ($n < 3$)**:** *When* $n = 1$, C_0 *can be covered if and only if* $C_1 = C_0$. *When* $n = 2$, C_0 *can be covered if and only if* $C_1 = C_0$ *or* $C_2 = C_0$. *In order to cover* R *twice, there are points which are covered by more than 3 tags. Therefore, we can omit this case from the consideration.*

Case 2 ($n \geq 3$)**:** *For the sake of symmetry, all neighboring tags have to appear on the circumference of the readable area of* v_0 *to minimize the number of neighboring tags. Let* v_1 *be on the circumference of the readable area centered at* v_0, *as shown in Figure 6. Let* A_0 *be the location of* v_0 *and* A_1 *be one of the intersections of two circles* C_0 *and* C_1. *To minimize 3-covering area, the circle of the second neighboring tag* v_2 *has to cross the two points* A_0 *and* A_1. *Hence,* v_2 *is on the circumference of the readable-area circle of* v_0 *and* $\angle v_1 A_0 v_2 = \frac{2}{3}\pi$. *Similarly, the third neighboring tag* v_3 *is also on the circumference of the circle of* v_0 *and* $\angle v_2 A_0 v_3 = \frac{2}{3}\pi$. *The three neighboring tags are enough to cover* C_0 *as*

15

$C_0 \subset C_1 \cup C_2 \cup C_3$, *and this setting minimizes the 3-covering area.*

Therefore, the hexagon pattern with edge length r is optimal for $k = 2$, as illustrated in Figure 4. This concludes the proof.

4.4. The Optimal Tag Deployment Pattern for $k = 3$

For $k = 3$, all points in the region need to be covered by the readable area of at least three tags. We observe that the diamond pattern with edge length r is optimal. Theorem 2 points out that with a given k value, minimizing the number of tags to be deployed is equivalent to minimizing the amount of area covered by more than k tags in the region R. By applying this theorem, the optimality of the diamond pattern is proved in the following.

Theorem 4 *The optimal 3-covering RFID tag deployment pattern is the diamond pattern with edge length r.*

Consider a set of tags $\{v_0, v_1, v_2, ..., v_n\}$ and their readable areas $\{C_0, C_1, C_2, ..., C_n\}$, which are depicted in Figure 7. Similar to the case of $k = 2$, the problem is how many neighboring tags are required to cover C_0 twice. From Theorem 3, we can see that at least three neighboring tags are required for $k = 3$. Thus we omit discussion for the case $n \leq 3$.

Due to the nature of symmetry, all neighboring tags have to appear on the circumference of the readable area of v_0 to minimize the number of neighboring tags. Let us put v_1 at a arbitrary point on the circumference of C_0. To cover C_0 twice, the intersection area $C_0 \cap C_1$ needs to be covered by other neighboring tags and they should also be on the circumference of C_0. When there is only one additional tag to cover $C_0 \cap C_1$, the tag has to be placed at the same point as tag v_1, which is not acceptable. Consequently, the minimum number of tags to cover

$C_0 \cap C_1$ is two. For example, in Figure 7, $C_0 \cap C_1$ is covered by $C_2 \cup C_3$. Finally, we derive that six neighboring tags are able to cover C_0 twice while at the same time minimizing the amount of areas covered by more than 3 tags. This concludes that the diamond pattern with edge length r is optimal for $k = 3$, which is depicted in Figure 8.
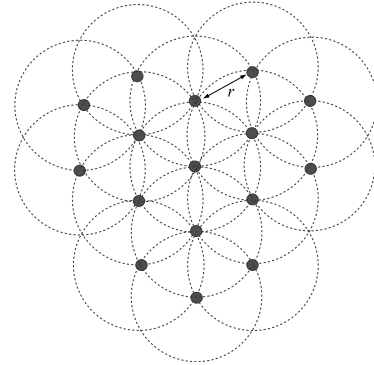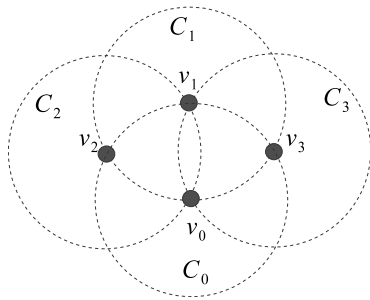

Figure 7: An example for the proof when $k = 3$.   Figure 8: The optimal pattern for $k = 3$.

4.5. The Square Deployment Pattern

In previous sections, we have presented the optimal k-covering tag deployment patterns for $k \in \{1, 2, 3\}$. However, in practice, the square pattern is employed in many applications (Liu et al., 2007; Munishwar et al., 2009b; Mitchell et al., 2009; Ota et al., 2008), because of the ease of deployment. Hence, in this section, we analyze the minimum number of tags required by the square pattern for k-covering, where $k \in \{1, 2, 3\}$.

Given a fixed k value, minimizing the number of tags N required by the square pattern can be seen as the special case of the optimal patterns. For $k = 1$, as shown in Figure 9, the readable areas of the top-left four tags intersect at point A_0, which

17

is the center of the four tags. Hence, when the edge length is $\sqrt{2}r$, the square pattern requires the minimum number of tags as illustrated in Figure 9.

For $k = 2$, according to Theorem 3, each tag has at least three neighboring tags. When each tag has four neighboring tags, the tags form the square pattern. Therefore, when the edge length is r, the square pattern requires the minimum number of tags to achieve 2-covering as shown in Figure 10.

For $k = 3$, Theorem 4 indicates that each tag needs to have at least six neighboring tags. When each tag has eight neighboring tags, the tags form the square pattern. Thus, when the edge length is $\frac{1}{\sqrt{2}}r$, the square pattern requires the minimum number of tags to achieve 3-covering, which is shown in Figure 11.
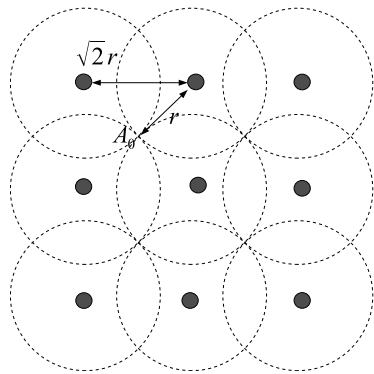

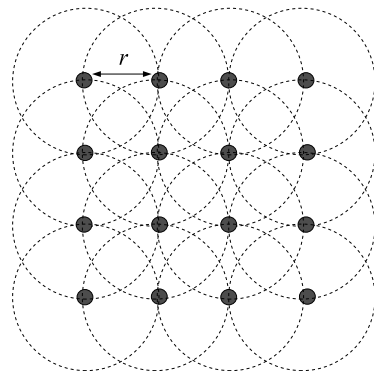Figure 9: The square pattern for $K = 1$.   Figure 10: The square pattern for $k = 2$.

5. Analysis

In this section, we provide analytical models for the upper bound and the average value of localization error.
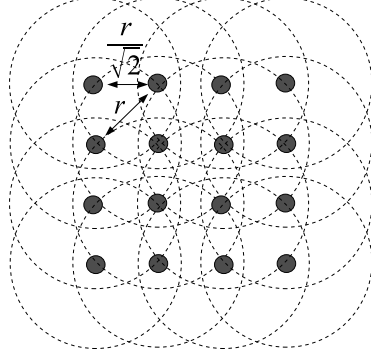
18

Figure 11: The square pattern for $k = 3$.

5.1. Analysis of the Upper Bound

In this section, we analyze the upper bound of localization error when the optimal deployment patterns are applied. If the real location of an RF reader is (x, y) and the estimated location is (x_e, y_e), the localization error Err is the Euclidean distance between them and can be computed by:

$$Err = \sqrt{(x - x_e)^2 + (y - y_e)^2} \tag{13}$$

Denoting the upper bound as Err_{up}, the error range is $[0, Err_{up}]$. The value of Err_{up} depends on what localization scheme is used. For example, in Figure 12 (a), a reader is in the readable area of tag v_i located at (x_i, y_i). If the reader randomly estimates its position by the uniform distribution, $Err_{up} = 2r$, as $0 \le (x_i - x)^2 + (y_i - y)^2 \le r^2$ and $0 \le (x_i - x_e)^2 + (y_i - y_e)^2 \le r^2$. The localization error reaches the upper bound when the distance between a reader and a tag is r and the reader estimates its location at the opposite side of the readable area, as shown in Figure 12 (a).

To improve the performance of localization, we are interested in the localization scheme which minimizes Err_{up}. Given the number of tags that a reader can
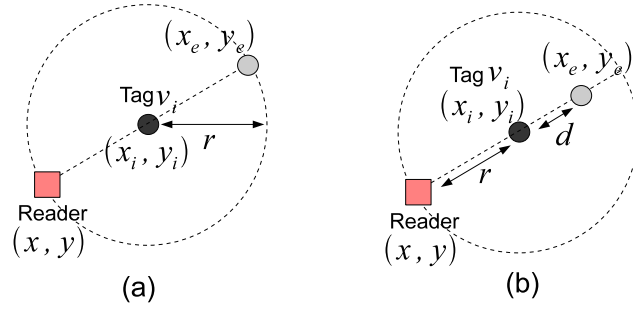
19

Figure 12: An example of localization error upper bound.

access, we define the achievable minimum upper bound of localization error as follows.

Definition 3 *When a reader estimates its location based on the positions of the accessible tags, the achievable minimum upper bound of localization error is defined by:*

$$\min_{\forall \ scheme} \{Err_{up}\} \tag{14}$$

The following Lemmas give the estimation of the achievable minimum upper bound of localization error.

Theorem 5 *When an RF reader detects exactly one tag, the achievable minimum upper bound of localization error is r.*

Proof 4 *Let (x_i, y_i) be the location of a tag which an RF reader can access. The real location of the reader (x, y) is randomly distributed within the readable area of the tag. In other words, $(x_i - x)^2 + (y_i - y)^2 \leq r^2$. Let d denote the distance between (x_i, y_i) and (x_e, y_e), and d is between $[0, r]$. By observing Figure 12 (b), we can clearly see that $Err_{up} = r + d$. When $d = 0$, Err_{up} reaches the minimum*

20

r. Therefore, the achievable upper bound of localization error is r. This concludes the proof.

Theorem 6 *When an RF reader detects more than one tag, the achievable minimum upper bound of localization error is half of the longest line drawn inside of the intersection area of readable areas of all accessible tags.*

Proof 5 *Let the line $\overline{A_1 A_2}$ be the longest line drawn inside of the intersection of readable areas of the detected k tags, and p be the middle point of the line. In addition, let $p_e = (x_e, y_e)$ be the estimate location of the RF reader computed from one of the localization schemes. It is reasonable for p_e to be inside of the intersection region. Assume $p_e \neq p$ and the distance between p_e and A_1 is d. This is illustrated in Figure 13. Notice that $\max(\angle p_e p A_1, \angle p_e p A_2) \geq \frac{\pi}{2}$. Without loss of generality, let $\angle p_e p A_1 \geq \frac{\pi}{2}$. This implies that $d > \frac{\|\overline{A_1 A_2}\|}{2}$. Now since the real location of the RF reader could be anywhere in the intersection region, Err_{up} will be d if the real location of the RF reader happens to be at A_1. In this case, $Err_{up} > \frac{\|\overline{A_1 A_2}\|}{2}$. To minimize Err_{up}, p_e should be assigned to the middle point of $\overline{A_1 A_2}$, and the achievable minimum upper bound of localization error is $\frac{\|\overline{A_1 A_2}\|}{2}$. This concludes the proof.*

Based on Lemmas 5 and 6, we can derive the optimal localization scheme with a given number of tags that a reader can detect to minimize the upper bound of localization error.

Corollary 7 *When an RF reader detects exactly one tag, the optimal localization scheme is to use the location of the detected tag as the estimated location. When an RF reader detects more than one tag, the optimal localization scheme is to*
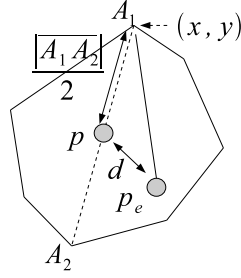
The intersection area of readable area of k tags

Figure 13: An example for the upper bound of localization error.

use the middle of the longest line in the intersection of the readable areas of all detected tags as the estimated location.

5.2. Average Localization Error when $k = 1$

When $k = 1$, depending on the location of the RF reader, it can access either one or two tags. It is not difficult to see that the intersection of two tags is $r^2(\angle A_1 v_1 A_2 - sin(\angle A_1 v_1 A_2))$, where $\angle A_1 v_1 A_2 = \pi/3$ when our optimal 1-covering tag deployment pattern is used, which is illustrated in Figure 14 (a). Note that the deployment pattern is an equilateral triangle, and thus the intersection of any two adjacent circles is the same. Let us denote the probability for a reader to access k tags as $P\{|E| = k\}$. The probability $P\{|E| = 1\}$ and $P\{|E| = 2\}$ can be obtained by the following formulas:

$$P\{|E| = 1\} = \frac{\pi r^2 - 6r^2(\pi/3 - \sqrt{3}/2)}{\pi r^2} \approx 0.654 \tag{15}$$

$$P\{|E| = 2\} = \frac{6r^2(\pi/3 - \sqrt{3}/2)}{\pi r^2} \approx 0.346 \tag{16}$$

22

Let X and Y be random variables that the real location of a reader is (x, y) with respect to accessible tags. The joint probability distribution function (pdf) of X and Y is given as follows.

$$f(x, y) = \begin{cases} \frac{1}{\pi r^2} & , x^2 + y^2 \leq r^2 \\ 0 & , otherwise \end{cases} \tag{17}$$

Let Z_k be the localization error when a reader can access k tags. The cumulative distribution function (cdf) of $Z_1 = X^2 + Y^2$ is obtained as follows.

For $0 \leq a \leq r$,

$$\begin{aligned} F_{Z_1}(a) &= P\{X^2 + Y^2 \leq a^2\} \tag{18} \\ &= \int\int_{x^2+y^2 \leq a^2} f(x, y) \, dxdy \tag{19} \\ &= \frac{a^2}{r^2} \tag{20} \end{aligned}$$

From the above equation, the pdf of Z_1 is:

$$f_{Z_1}(a) = \frac{d}{da} F_{Z_1}(x) = \frac{2a}{r^2} \tag{21}$$

Hence, the expected value of Z_1 is:

$$E[Z_1] = \int_0^r x f_{Z_1}(x) dx = \frac{2}{3} r \tag{22}$$

When a reader can access two tags, the pdf of X and Y is given as follows.

For $\frac{\sqrt{3}}{2} r \leq X \leq r$ and $0 \leq Y \leq \frac{1}{2} r$,

$$f(x, y) = \begin{cases} \frac{4}{r^2(\pi/3 - \sqrt{3}/2)} & , (x - \frac{\sqrt{3}}{2} r)^2 + y^2 \leq (\frac{1}{2} r)^2 \\ 0 & , otherwise \end{cases} \tag{23}$$

23

The cdf of $Z_2 = (X - \frac{\sqrt{3}}{2}r)^2 + Y^2$ is obtained as follows.

For $0 \le a \le \frac{1}{2}r$,

$$
\begin{aligned}
F_{Z_2}(a) &= P\{(X - \frac{\sqrt{3}}{2}r)^2 + Y^2 \le a^2\} & (24) \\
&= \int\int_{(X - \frac{\sqrt{3}}{2}r)^2 + Y^2 \le a^2} f(x,y)\, dxdy & (25) \\
&= \frac{\pi a^2}{16r^2(\pi/3 - \sqrt{3}/2)} & (26)
\end{aligned}
$$

The pdf of Z_2 is:

$$
f_{Z_2}(a) = \frac{d}{da} F_{Z_2}(a) = \frac{\pi a}{8r^2(\pi/3 - \sqrt{3}/2)} \tag{27}
$$

Hence, the expected value of Z_2 is:

$$
\begin{aligned}
E[Z_2] &= \int_0^{\frac{1}{2}r} x f_{Z_2}(x) dx & (28) \\
&= \frac{\pi r}{192(\pi/3 - \sqrt{3}/2)} & (29)
\end{aligned}
$$

Therefore, when $K = 1$, the average localization error is as follows.

$$
\begin{aligned}
\overline{Err_1} &= \sum_{i=\{1,2\}} P\{|E| = i\} \cdot E[Z_i] & (30) \\
&\approx 0.46714r & (31)
\end{aligned}
$$

5.3. Average Localization Error when $k = 2$

When $k = 2$, a reader can access either two or three tags. As the size of a 3-covering area among three adjacent circles is $r^2(\pi/3 - sin(\pi/3))$, through the

24

observation of Figures 4 and 14, $P\{|E| = 2\}$ and $P\{|E| = 3\}$ can be obtained as follows.

$$P\{|E| = 2\} = \frac{\pi r^2 - 9r^2(\pi/3 - sin(\pi/3))}{\pi r^2} \approx 0.481 \tag{32}$$

$$P\{|E| = 3\} = \frac{9r^2(\pi/3 - sin(\pi/3))}{\pi r^2} \approx 0.519 \tag{33}$$

The expected localization error can be calculated in a similar manner to the case of $k = 1$. The differences between the cases of $k = 1$ and $k = 2$ are the upper bound of Z_k and the distance between two adjacent tags. As shown in Figure 14 (b), if a reader can access two tags, $\angle A_1 v_1 A_2 = 2\pi/3$. The pdf of X and Y is given as follows.

For $\frac{1}{2}r \le X \le r$ and $0 \le Y \le \frac{\sqrt{3}}{2}r$,

$$f(x, y) = \begin{cases} \frac{4}{r^2(2\pi/3 - \sqrt{3}/2)} & , (x - \frac{\sqrt{3}}{2}r)^2 + y^2 \le (\frac{\sqrt{3}}{2}r)^2 \\ 0 & , otherwise \end{cases} \tag{34}$$

The cdf of $Z_2 = (X - \frac{1}{2}r)^2 + Y^2$ is obtained as follows.
For $0 \le a \le \frac{\sqrt{3}}{2}r$,

$$\begin{aligned} F_{Z_2}(a) &= P\{(X - \frac{1}{2}r)^2 + Y^2 \le a^2\} & (35) \\ &= \int \int_{(x - \frac{1}{2}r)^2 + y^2 \le a^2} f(x, y) \, dxdy & (36) \\ &= \frac{\pi a^2}{r^2(2\pi/3 - \sqrt{3}/2)} & (37) \end{aligned}$$

The pdf of Z_2 is as follows.

25

$$f_{Z_2}(a) = \frac{d}{da} F_{Z_2}(a) = \frac{2\pi a}{r^2(2\pi/3 - \sqrt{3}/2)} \tag{38}$$

Hence, the expected value of Z_2 is as follows.

$$E[Z_2] = \int_0^{\frac{\sqrt{3}}{2}r} x f_{Z_2}(x) dx \tag{39}$$

$$= \frac{\sqrt{3}\pi r}{4(2\pi/3 - \sqrt{3}/2)} \tag{40}$$

When a reader can access three tags, $\angle A_1 v_1 A_2 = \frac{1}{3}\pi$ and $0 \le Z_3 \le \frac{1}{2}r$ (Figure 14 (c)). Hence, the expected value of Z_3 is very close to Equation 29.

$$E[Z_3] \approx \frac{\pi r}{192(\pi/3 - \sqrt{3}/2)} \tag{41}$$

Therefore, when $K = 2$, the average localization error is obtained as follows.

$$\overline{Err_2} = \sum_{i=\{2,3\}} P\{|E| = i\} \cdot E[Z_i] \tag{42}$$

$$\approx 0.224r \tag{43}$$

5.4. Average Localization Error when $k = 3$

When $k = 3$, an RF reader can access either three or four tags. Because the size of a 4-covering area among four adjacent circles is $r^2(\pi/3 - sin(\pi/3))$, from the observation of Figure 8, $P\{|E| = 3\}$ and $P\{|E| = 4\}$ can be calculated as follows.

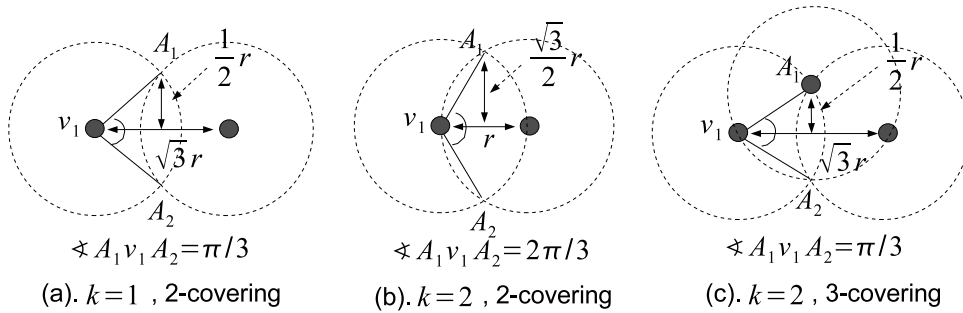$$P\{|E| = 3\} = \frac{\pi r^2 - 12r^2(\pi/3 - sin(\pi/3))}{\pi r^2} \approx 0.309 \tag{44}$$

26

Figure 14: Examples for the average localization error.

$$P\{|E| = 4\} = \frac{12r^2(\pi/3 - sin(\pi/3))}{\pi r^2} \approx 0.691 \tag{45}$$

When a reader is able to access three tags, the computation of the average localization error is complicated due to the shape of the intersection of readable areas of tags, which is illustrated in Figure 15 (a). Thus, we approximate the average localization error by assuming that points (x_e, y_e), v_1, and v_2 comprise a sector of a circle with radius $\pi/\sqrt{3}$ as demonstrated in Figure 15 (b). Using this approximation, the pdf can be obtained as follows.

$$f(x, y) = \begin{cases} \frac{3}{\pi r^2} & , x^2 + y^2 \leq \frac{1}{\sqrt{3}}r \\ 0 & , otherwise \end{cases} \tag{46}$$

The cdf of $Z_3 = X^2 + Y^2$ is as follows.

$$
\begin{aligned}
F_{Z_3}(a) &= P\{X^2 + Y^2 \leq a^2\} \tag{47}\\
&= \int\int_{x^2+y^2\leq a^2} f(x, y)\, dxdy \tag{48}\\
&= \frac{3a^2}{r^2} \tag{49}
\end{aligned}
$$

27

The pdf of Z_3 is as follows.

$$f_{Z_3}(a) = \frac{d}{da} F_{Z_3}(a) = \frac{6a}{r^2} \tag{50}$$

Hence, the expected value of Z_3 is as follows.

$$E[Z_3] = \int_0^{\frac{1}{\sqrt{3}}r} x f_{Z_3}(x) dx = \frac{2}{3\sqrt{3}} r \tag{51}$$

If a reader can access four tags (Figure 15 (c)), the average localization error is exactly the same as that of the case when $k = 3$ and $|E| = 3$, which is shown in Figure 14 (c). Hence, the expected value of Z_4 is:

$$E[Z_4] \approx \frac{\pi r}{192(\pi/3 - \sqrt{3}/2)} \tag{52}$$

Therefore, when $k = 3$, the average localization error is obtained by the following formula.

$$\overline{Err_3} = \sum_{i=\{3,4\}} P\{|E| = i\} \cdot E[Z_i] \tag{53}$$

$$\approx 0.181r \tag{54}$$

6. Performance Evaluation

In this section, numerical results are provided to compare the performance of the optimal k-covering deployment patterns when $k \in \{1, 2, 3\}$ with the corresponding square pattern. In addition, extensive simulations implemented in Java programming language are conducted to compare the results with our analytical models. Our simulation environment consists of a number of RF tags deployed in
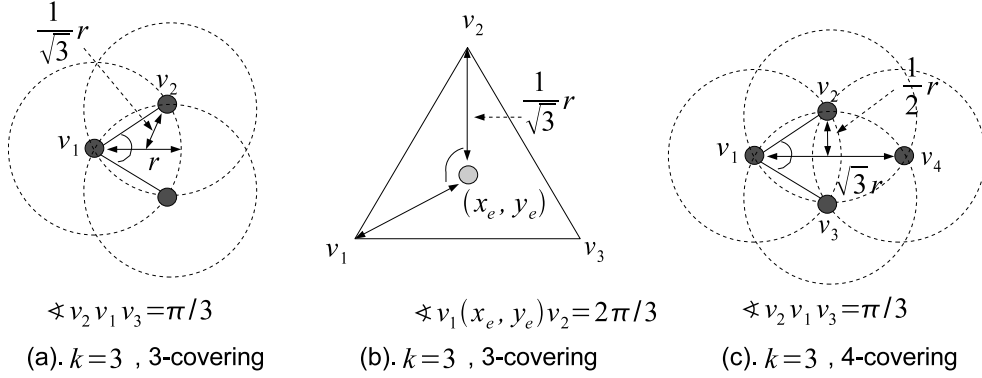
Figure 15: Examples for the average localization error.

a $10m$ by $10m$ square region. The backward channel range varies from $0.1m$ to $1m$, and the forward channel range is assumed to always be larger than the backward channel range. Consequently, the communication range r is between $0.1m$ and $1m$.

To evaluate the performance of the deployment patterns, we employ two metrics: the number of required tags and the relative tag density. The number of required tags is defined as the total number of tags to be deployed in the region. Denoting N_{opt} as the number of tags required by the optimal pattern and N_{square} as that required by the square pattern, the relative tag density is defined as $\frac{N_{opt}}{N_{square}}$.

6.1. Numerical Results

Figure 16 shows the number of required tags and the relative tag density with respect to the communication range, when $k = 1$. Because the equilateral triangle pattern is optimal when $k = 1$, it always requires smaller amount of tags to be deployed than that of the square pattern. As demonstrated in the right-hand vertical axis, the relative tag density is about 0.77. This indicates that the equilateral

triangle pattern is able to save around 23% of the amount of RF tags compared with the square pattern.

Figure 17 illustrates the number of required tags and the relative tag density with respect to the communication range when $k = 2$. It is clear that the optimal pattern (i.e., the hexagon pattern) results in fewer required tags than the square pattern. The number of tags required by the hexagon pattern is approximately 87% of the amount of tags required by the square pattern.

Figure 18 presents the number of required tags and the relative tag density with respect to the communication range when $k = 3$. Compared with the square pattern, the diamond pattern requires only 58% of the amount of tags to achieve 3-covering. According to the results, the optimal diamond pattern significantly outperforms the square pattern. Based on Figures 16, 17, and 18, the optimal k-covering tag deployment patterns improve tag usage efficiency for $k \in \{1, 2, 3\}$. Note that the relative tag density first increases from 0.77 to 0.87 when the value of k increases from 1 to 2 and then decreases from 0.87 to 0.58 when the value of k increases from 2 to 3. This is because that in some cases the square pattern could be close to the optimal pattern. In other words, the relative tag density could be a good metric to evaluate different tag deployment patterns.

6.2. Comparisons between Simulation and Analytical Results

In this section, we compare the simulation and analytical results of the optimal tag deployment patterns. We do not compare the optimal patterns with the square pattern. Since the square pattern deploys more tags, it will lead to lower localization error, but such comparisons would be unfair.

Figure 19 demonstrates localization error in respect to communication range when the equilateral triangle pattern is applied for 1-covering. It is clear that the
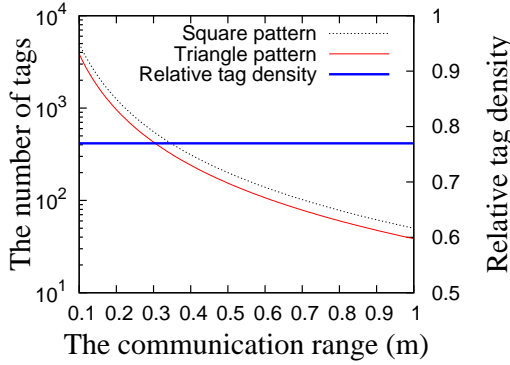
30

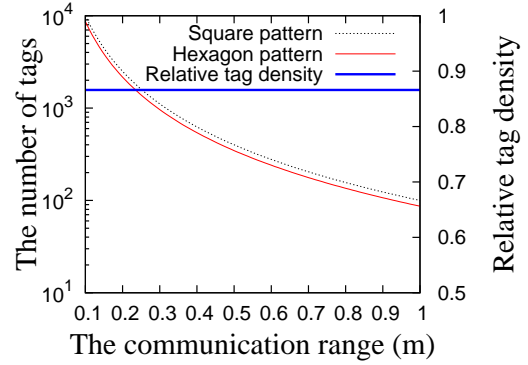Figure 16: The number of tags ($K = 1$).
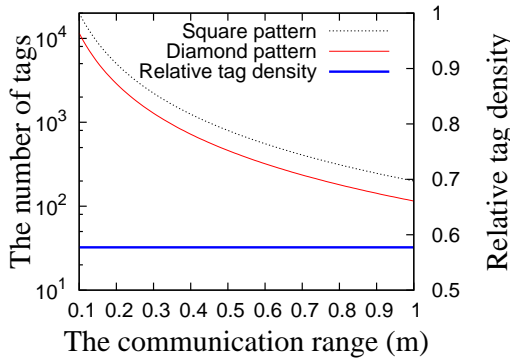

Figure 17: The number of tags ($K = 2$).
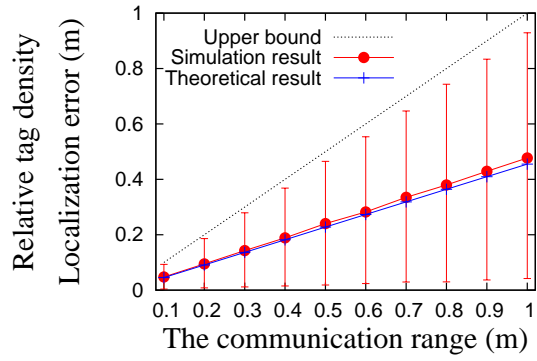

Figure 18: The number of tags ($K = 3$).

Figure 19: The localization error ($K = 1$).

localization error increases as the communication range expands. As can be seen from Figure 19, the simulation and analytical results are very close to each other.

Figure 20 shows localization error against communication range when the hexagon pattern is applied for $k = 2$. The average localization error is much lower than the upper bound, because there exists a portion of 3-covering area in region R.

Figure 21 illustrates the localization error with respect to the communication range when the diamond pattern is applied for $k = 3$. As shown in the figure, the
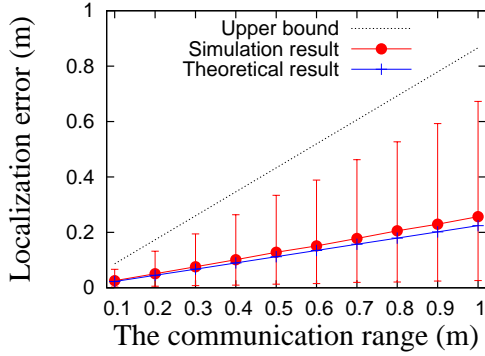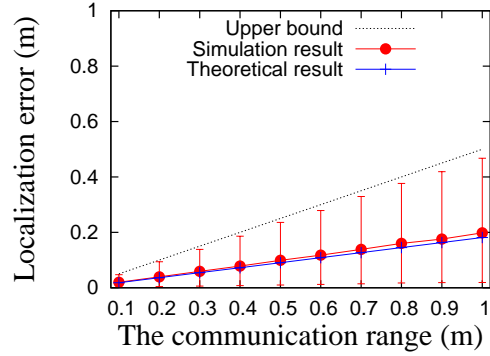
Figure 20: The localization error ($K = 2$).

Figure 21: The localization error ($K = 3$).

localization error is small enough to support most RFID-based applications.

As reported by Figures 19 to 21, our analytical models are validated and they provide very accurate estimations.

Table 2: Percentage of localization error.

k	% of error
1	Up to 2.58%
2	Up to 3.28%
3	Up to 1.91%

Table 2 presents the percentage of localization errors between simulation and analytical results, which is defined by $(Err_{sim} - Err_{analysis})/r$, where Err_{sim} and $Err_{analysis}$ are the average of localization errors by simulations and analytical models, respectively. As can be seen in Table 2, our analytical models provide very close estimation of localization errors.

7. Conclusion

A new type of RFID-based applications, such as activity monitoring and localization, have been proposed in recent years. In these applications, RF tags are deployed on the ground instead of being attached to objects. However, the problem of the optimal tag deployment pattern for localization has yet to be addressed. In this paper, we define the optimal RFID tag deployment problem, which is to minimize the number of tags to be deployed in a region with a given minimal number of tags, k, that a reader can access at any point in the region. We analyze the achievable minimum upper bound of localization error when our optimal patterns are applied. We have shown that the localization error is upper bounded by r when $k = 1$, by $\frac{\sqrt{3}}{2}r$ when $k = 2$, and by $\frac{1}{2}r$ when $k = 3$. In addition, the analytical models for the average localization error are built for the three aforementioned k values. To evaluate the performance, we conduct both numerical analysis and computer simulations. The numerical results show that the optimal patterns require only 77%, 87%, and 58% of the amount of tags which are required by the commonly used square pattern, when the value of k is 1, 2, and 3, respectively. The comparison between simulation and analytical results has demonstrated that our analytical models provide very accurate estimations of localization error.

References

Bai, X., Kumar, S., Xuan, D., Yun, Z., Lai, T.-H., 2006. Deploying Wireless Sensors to Achieve both Coverage and Connectivity. In: Proceeding of the Interational Symposium on Mobile Ad Hoc Networking and Computing (MobiHoc). pp. 131–142.

Bai, X., Xuan, D., Yun, Z., Lai, T.-H., Jia, W., 2008. Complete Optimal Deployment Patterns for Full-Coverage and k-Connectivity (k<=6) Wireless Sensor Networks. In: Proceeding of the Interational Symposium on Mobile Ad Hoc Networking and Computing (MobiHoc). pp. 401–410.

Boss, R. W., 2003. RFID Technology for Libraries. Library Technology Reports (Chicago: American Library Association).

Choi, J.-W., Oh, D.-I., Kim, S.-W., 2006. CPR Localization Using the RFID Tag-Floor. In: Proceedings of the Pacific Rim International Conference on Artificial Intelligence (PRICAI). pp. 870–874.

Chow, H. K. H., Choy, K. L., Lee, W. B., Lau, K. C., 2006. Design of a RFID Case-based Resource Management System for Warehouse Operations. Expert Systems with Applications 30 (4), 561–576.

iRobotCreate, 2009. http://store.irobot.com/.

Jin, G., Lu, X.-Y., Park, M.-S., 2006. An Indoor Localization Mechanism Using Active RFID Tag. In: Proceedings of the IEEE International Conference on Sensor Networks, Ubiquitous, and Trustworthy Computing (SUTC). pp. 40–43.

Kershner, R., 1939. The Number of Circles Covering a Set. American Journal of Mathmatics 61, 665–671.

Liu, Y., Chen, L., Jian, P., Chen, Q., Zhao, Y., 2007. Mining Frequent Trajectory Patterns for Activity Monitoring Using Radio Frequency Tag Arrays. In: Proceedings of the IEEE International Conference on Pervasive Computing and Communications (PerCom). pp. 37–46.

Mitchell, C., Munishwar, V., Singh, S., Wang, X., Gopalan, K., Abu-Ghazaleh, N., 2009. Testbed Design and Localization in MiNT-2: A Miniaturized Robotic Platform for Wireless Protocol Development and Emulation. In: Proceeding of the International Conference on Communication Systems and Networks (COMSNETS).

Munishwar, V., 0003, S. S., Mitchell, C., Wang, X., Gopalan, K., Abu-Ghazaleh, N. B., 2009a. Rfid based localization for a miniaturized robotic platform for wireless protocols evaluation. In: Proceedings of the IEEE International Conference on Pervasive Computing and Communications (PerCom). pp. 1–3.

Munishwar, V., Singh, S., Mitchell, C., Wang, X., Gopalan, K., Abu-Ghazaleh, N., 2009b. On the Accuracy of RFID-based Localization in a Mobile Wireless Network Testbed. In: Proceeding of the IEEE PerCom Workshop on Pervasive Wireless Networking.

Ota, Y., Hori, T., Onishi, T., Wada, T., Mutsuura, K., Okada, H., 2008. An Adaptive Likelihood Distribution Algorithm for the Localization of Passive RFID Tags. IEICE Transaction on Fundamental Electronics Commununications Computer Science E91-A (7), 1666–1675.

Santos, B. L. D., Smith, L. S., 2008. RFID in the Supply Chain: Panacea or Pandora's Box. Commun. ACM 51 (10), 127–131.

Want, R., 2004. The magic of rfid. ACM Queue 2 (7), 40–48.

Xie, J., Yang, J., Chen, Y., Wang, H., Yu, P. S., 2008. A Sampling-Based Approach to Information Recovery. In: Proceedings of the International Conference on Data Engineering (ICDE). pp. 476–485.

Zhang, H., Hou, J., Mar. 2005. Maintaining Sensing Coverage and Connectivity in Large Sensor Networks. Ad Hoc and Sensor Wireless Networks 1 (1-2), 89–124.